We are IntechOpen, the world's leading publisher of Open Access books Built by scientists, for scientists

6,900
Open access books available

185,000
International authors and editors

200M
Downloads

Our authors are among the

154
Countries delivered to

TOP 1%
most cited scientists

12.2%
Contributors from top 500 universities



WEB OF SCIENCE™

Selection of our books indexed in the Book Citation Index in Web of Science™ Core Collection (BKCI)

Interested in publishing with us?
Contact book.department@intechopen.com

Numbers displayed above are based on latest data collected.
For more information visit www.intechopen.com



15

Biometric Application in Fuel Cells and Micro-Mixers

Chin-Tsan Wang
National I Lan University
Taiwan

1. Introduction

1.1 Fuel cells related

Over the past few decades, there has been a growing interest in the fuel cell system of power generation and micro-mixers because it has been widely applied in mobile and microfluidic systems, respectively. Regarding the fuel cell systens, Proton Exchange Membrane Fuel Cells (PEMFC) seem to be one of the better solutions for a vehicular power source in the future due to their high power density, solid electrolytes, low corrosion and low-temperature operation. However, some issues are still of concern, in particular the cost, the size, the weight and the complexity of peripheral devices (Marsala et al., 2009). Bipolar plates are one of the most important and expensive components of PEM fuel cells. This is because they account for more than 60% of the total weight and 30% of the total cost of the system. Therefore, improving or addressing a novel flow slab design seems to be workable for improving these issues with respect to weight, volume and cost.

From past studies, it is known that the uniformity of oxygen distribution in cathode channels significantly affects the performance of PEM fuel cells. Different types of flow-fields have been addressed and studied to improve power performance (Mei et al., 2006; Weng et al., 2005; Yan et al., 2008). Results show that increasing the fuel rate (Mei et al., 2006) and higher flow field uniformity (Weng et al., 2005; Yan et al., 2008) are useful to the performance of fuel cells. In addition, pressure drop would be one of the important factors for flow-field design because it can simultaneously cause an excess of motor power dissipation (Yan et al., 2007). In other aspects, the aspect ratio of the channel would also simultaneously affect the pressure drop and even the cell performance (Perng et al., 2009). Also of importance, the new flow slab designs originating from bionic features, addressed by Kloess et al., (2009) and Wang et al., (2009), are of significance to fuel cells but have rarely been noted. A biophysical flow slab design, created to mimic features of vascular flow networks, was employed by Wang et al., (2009) due to its excellent performance in the uniformity of flow distribution and lower pressure drop. Latterly, two new types of biometric flow slab, namely BFF1 and BFF2, originating from the prototype type were addressed by Wang et al., (2009) and confirmed by the performance of the cells (Wang et al., 2010).

Furthermore, it has been also extended to the study of microbial fuel cells to enable the improvement of power performance, (Chen, 2010), because of the desire for clean energy. The development of processes by which to generate biofuels and bioenergy have been of

special interest of late. Among these, microbial fuel cells have received increased attention. This process, which collects the electricity generated by microbes when they metabolize substrates, is considered to be one of the most efficient energy sources because no burning is required to produce energy (Watanabe, 2008). Also, the only raw materials needed to power fuel cells are simple organic compounds or even waste materials from other reactions (Watanabe, 2008; Lovely, 2008). There are still many obstacles that need to be overcome before this technology can be put to use. Currently the voltage and amperage generated by microbial fuel cells is so low that they have no useful applications (Watanabe, 2008; Lovely, 2008). In order to develop solutions to these problems, research is being done to engineer more efficient hardware for fuel cells in addition to understanding how different microbes interact with the anodes/cathodes when transporting electrons (Lovely, 2008; Bergel et al., 2008). As for the flow slab design of MFCs, there is an absence of sufficient discussion and research regarding the design of the flow channel and flow field (Hameler et al., 2006; Logan et al., 2004), and even less discussion as to why and how they could be applied to MFCs. However, a biometric flow channel applied to rumen microbial fuel cells (RMFCs) was first addressed by Chen (2010).

1.2 Passive micro-mixer related

A biometric concept could also be applied to the design of a passive micro-mixer because it is simple to operate and provides an excellent mixing performance under the condition of lower pressure (Wang et al., 2009). Recently, microfluidics have received a lot of attention in the development of automated miniaturized analytical devices in (bio)analytical chemistry. Microfluidics deals with microscale, physical phenomena of fluid and particle flows in microchannels that connect various functional sites on a miniaturized analytical device. Among the various functionalities, rapid mixing is crucial because biological analyses, like enzyme reactions, protein folding, and cell activation, require a rapid reaction process that can be controlled by the mixing of reactants. Unfortunately, mixing at a microscale mainly depends on molecular diffusion, resulting in an extremely slow process and long microchannel for complete mixing. This is because almost all microchannel flows are laminary, and the Reynolds number is so slow that turbulent mixing is hard to be achieved (Song et al., 2006).

As for micro-mixers, application fields of microchannel-based mixers encompass both modern, especialised issues such as sample preparation for chemical analysis in addition to the traditional, widespread usable mixing tasks, such as reaction, gas absorption, emulsification, foaming and blending (Bayer et al., 2003; Ehrfeld et al., 2000; Hessel et al., 2004; Jensen, 1998; Lowe et al., 2000). Moreover, they are suitable for integration with other devices.

Many passive micro-mixers have been developed in order to enhance and control mixing in a microchannel (Nquyen and Wu, 2005). A passive mixer uses special geometries embedded in a microchannel, such as grooves, rivets or posts, to increase the vorticity and, subsequently, to cause a chaotic advection (Johnes and Aref, 1998). Another type of passive mixer is the lamination mixer, which decreases the diffusion length and increases the contact area of fluids by splitting incoming streams into multiple substreams, and then laminating them into one stream again (Kamholz and Yager, 2002).

Concerning the most traditional passive micro-mixers, they have been constructed with straight fluid channels and designed with a combination of fillisters and/or fold paths to

enhance the mixing effect (Wong et al., 2003). However, the design of a straight channel requires a longer length to achieve the goal of uniform mixing. Hence, it is always associated with the problems of mixer size and full-field inspection. In addition, fluid mixing at the microscopic scale is far more difficult than that in macroscopic fluid devices. In a typical microfluidic device, viscosity dominates the flow and the fluid streams prefer to adopt laminar flow patterns. Thus, fluid mixing that depends primarily on molecular diffusion is very slow. To achieve optimal mixing, an efficient passive micro-mixer usually involves complex 3-dimensional geometries, which are utilized to enhance the fluid lamination, stretching and folding. As mentioned above, mixing in the passive micro-mixer occurs with the diffusion of molecules in the microsystem and the process is very slow. Therefore, the complex geometry, or long microchannel, should be utilized for efficient mixing, but would cause a large pressure drop and difficulties in the design and fabrication process. In order to overcome this, a biophysical micro-mixer that originates from the biometric concept with a higher flow uniformity and lower pressure drop would be utilized by Wang et al., (2009) to provide better flow mixing within a limited device.

2. Biometric concept applied to fuel cells

2.1 Fuel cell bionic flow slab design (Wang et al., 2009)

Fuel cells possessing high potency and low pollution are well-known and considered the new generation of power technology. However, fuel cell performance and efficiency must be improved. The cost, reliability, and safety issues must be considered in the realization of commercial fuel cells. To enhance fuel cell performance and reliability, it is necessary to learn more about the mechanisms that cause performance losses. These include non-uniform concentrations, current density distributions, high ionic resistance due to dry membranes, and high diffusive resistance due to cathode flooding. The flow field and water/thermal management fuel cells require optimal designs to achieve high performance and reliability.
Flow-field plate design is one of the most significant factors that affects fuel cell efficiency.
This work presents a novel bionic concept flow slab design, which is shown in Figure 1, to improve fuel cell performance and compare it with other known flow slabs.
The variations in velocity and pressure drop uniformity are influenced by the wall effect and alter fuel cell performance. An index of the aspect ratio defined as AR=*D/L* was employed for 3D simulations at Re=10 and 100. Here, *D* is the flow channel depth and *L* is the flow channel width. Although flow field plate design is one of the most significant factors in fuel cell efficiency, the simultaneous effect of velocity uniformity and pressure drop on the performance of the system has rarely been examined. In this work, an index χ was used to quantitatively address the coupling effect between the velocity uniformity and pressure drop in the flow slab, as defined in (1):

$$\chi = \left(\frac{SD}{\mathrm{SD_p}} + \frac{\mathrm{PD}}{\mathrm{PD_p}}\right)^{-1} \tag{1}$$

where SD and PD indicate the standard deviation and pressure drop, respectively. The subscript p denotes that it is the value for parallel flow design, which is used as the basis when taking the ratio of the standard deviation and pressure drop. Therefore, when the value of χ is larger, fuel cell performance is better.

Numerical results obtained show that this novel biometric flow slab design will exhibit a better performance than traditional flow slabs, regardless of Reynolds numbers and aspect ratios, as it possesses a more uniform velocity and a lower pressure drop. Furthermore, the performance in the biometric flow slab's reaction area was determined to be superior (shown in Tables 1 and 2). Hence, increasing the bionic flow slab performance is worth investigation in order to obtain an optimal design, and the required numbers of inlet and outlet channels need to be studied. Different inlet and outlet numbers influence the velocity distribution and pressure drop variations, resulting in an integral performance. Two inlet channels and three outlet channels are suggested for the optimal bionic flow slab design. These findings show that the bionic concept and flow slab design addressed in this paper will be useful in enhancing fuel cell performance (Wang et al., 2009).

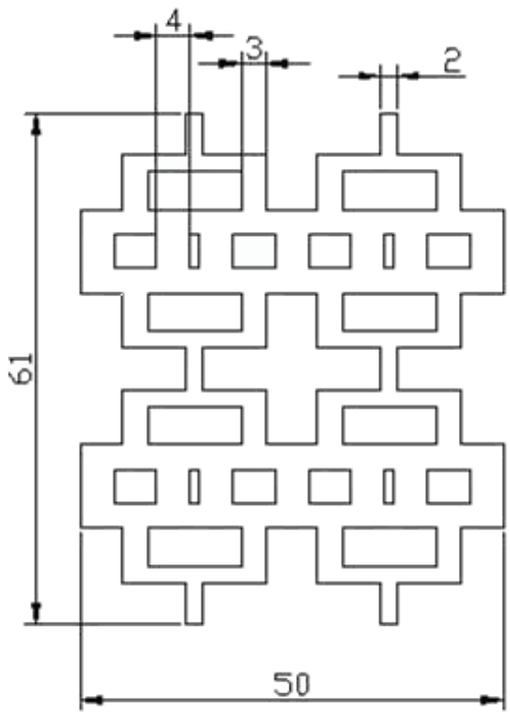


Fig. 1. Prototype of Biometric Flow Slab (unit: mm). Source: Wang et al., (2009)

	Parallel	Bionic	Net	Serpentine
χ	0.5	0.479	0.325	0.027
A_{Rea}	0.001438	0.001324	0.001	0.001512
χ / A_{Rea}	347.7	361.78	325	17.857

Table 1. Performance Index Versus Four Kinds of Flow Slabs at Re=10. Source: Wang et al., (2009)

	Parallel	Bionic	Net	Serpentine
χ	0.5	0.535	0.372	0.046
A_{Rea}	0.001438	0.001324	0.001	0.001512
χ / A_{Rea}	347.7	404.08	372	30.423

Table 2. Performance Index Versus Four Kinds of Flow Slabs at Re=100. Source: Wang et al., (2009)

2.2 Biometric flow slab applied to PEMFC (Wang et al., 2010)

As for the bipolar plates, they are one of the most important and expensive components of PEM fuel cells because they account for more than 60% of the total weight and 30% of the total cost of the system. Therefore, improving or addressing a novel flow slab design seems to be workable to improve these issues with respect to the weight, volume and cost. In this work, two kinds of novel biophysical flow slabs, namely BFF1 and BFF2, originating from the prototype of the biophysical flow slab shown in Figure 1, and due to their possession of a lower pressure drop and excellent flow uniformity, (Wang et al., 2009) shown in Figures 2 and 3,would be utilized in PEMFCs (Wang et al., 2010). They would then be compared with the two convectional flow slabs, the serpentine and parallel, which would be used for the investigation of cell performance.

The *I*–*V* cell polarization curves and *I*–*W* cell power density curves of the parallel, serpentine and two new biometric flow slabs were the first investigated and are shown in Figure 4. The results in Figure 4 show that serpentine and two biometric flow slabs (BFF1 and BFF2) have the appearance of a better performance than that of the parallel flow slab. The limited current densities at V_{cell}=0.27 for the serpentine, BFF1, and BFF2 compared with the parallel flow slab are increased by the amount of 58.19%, 58.48%, and 57.13%, respectively. When the operating voltage is lower than 0.57V, the performance of the parallel flow field seems to increase much more slowly than other flow slabs. This is because of its strong dependence on the distribution of the oxygen mass flow rate at the cathode GDL–CL interface, and a high oxygen mass flow rate will cause more oxygen to enter the CL for the electrochemical reaction.

Figure 5 shows the distribution and relation between the oxygen and liquid water at the three segments C-C1, C2-C3 and C4-C5 for BFF1. As the oxygen mass flow rate increases, the amount of liquid water from inlet to outlet decreases. The amounts of oxygen at the cross-section C-C1 and C4-C5 are less than C2-C3, resulting in lower current densities. Some baffles could be used and applied to promote the mass transport of C-C1 and C4-C5 in future studies (Perng et al., 2009).

Figure 6 indicates clearly that the BFF1 flow slab will produce a higher uniform distribution of current densities at the section of C-C1, C2-C3 and C4-C5. Hence, a higher performance for BFF1 would be expected because a higher uniform distribution of current density is one of the important factors for promoting the cell performance. Generally speaking, the lower the pressure loss is, the higher the net performance of the cell will be (Perng et al., 2009). To design a flow slab with a lower pressure drop, new flow slabs, named BFF1 and BFF2 respectively, were designed by the biophysical conception in this study.

Figure 7 displays the distribution and relation between oxygen and liquid water at the cross-sections of D-D1, D2-D3, D4-D5 and D6-D7 for BFF2. The trend of oxygen and liquid water distribution of D-D1, D2-D3, D4-D5 referred to are similar to C-C1, C2-C3 and C4-C5 of BFF1. The average oxygen distribution at the section of D6-D7, resulting from the shear stress, would be found to be the highest. Figure 8 shows that BFF2 would possess a better uniformity of flow distribution than BFF1. In addition, the shear stress would push more oxygen into CL for an electrochemical reaction, thus a greater current at the cross-section of D6-D7 could then be produced.

In this study, a pressure drop loss with respect to power density (Perng et al., 2009), defined in Equation (2), would be used to acquire a superior flow slab.

$$W_p = \frac{\Delta P A_{cha} V}{A_{total}} \tag{2}$$

In this equation, W_p represents the cathode pressure drop loss, ΔP is the total cathode pressure drop of the fuel cell, A_{cha} is the cross-sectional inlet flow area of cathode, V is the fuel velocity at the inlet of cathode, and A_{total} is the reaction area. The pressure drop losses of the cathode and output power of the cell, with respect to a parallel, serpentine, BFF1 and BFF2 flow slab, would be calculated and listed in Table 3. Due to a high pressure drop in channels, the W_{net} of serpentine is lower than that of the BFF2 in spite of the fact that the W_{cell} of serpentine is higher than that of BFF2. In addition, the pressure drop of BFF2 is lower than that of BFF1. Hence, the net power of the four kinds of flow slab would be obtained and shown in Table 3. It shows that the novel biometric flow slab of BFF1 and BFF2 would have a better performance than that of the serpentine and parallel flow slabs (Wang et al., 2010).

To sum up, the total pressure drop and the uniformity of flow distribution are two important factors for flow slab design because of their significant influence on the performance of the PEMFC. In this study, the two biometric flow slabs, BFF1 and BFF2, addressed in this study would have a better cell performance than the serpentine and parallel flow slabs because they possess a higher uniformity of flow distribution and a stronger ability to remove the liquid water. The novel biometric flow slab would have an enhanced cell power performance compared to the serpentine and parallel flow slabs. These findings, with respect to biometric flow slabs, would be useful to improve the PEMFC and could even be expanded to other cell types. (Wang et al., 2010).

Flow field type	$\triangle P$ (Pa)	W_{cell} (w/m²)	W_p (w/m²)	W_{net} (w/m²)
Parallel	248	3529	4.4	3524.6
Serpentine	5137	5583	91	5492
BFF1	2073	5593	37	5557
BFF2	730	5546	13	5533

Table 3. Estimation of Pressure Drop Losses at an Operating Voltage of 0.27V.
Source: Wang et al., (2010)

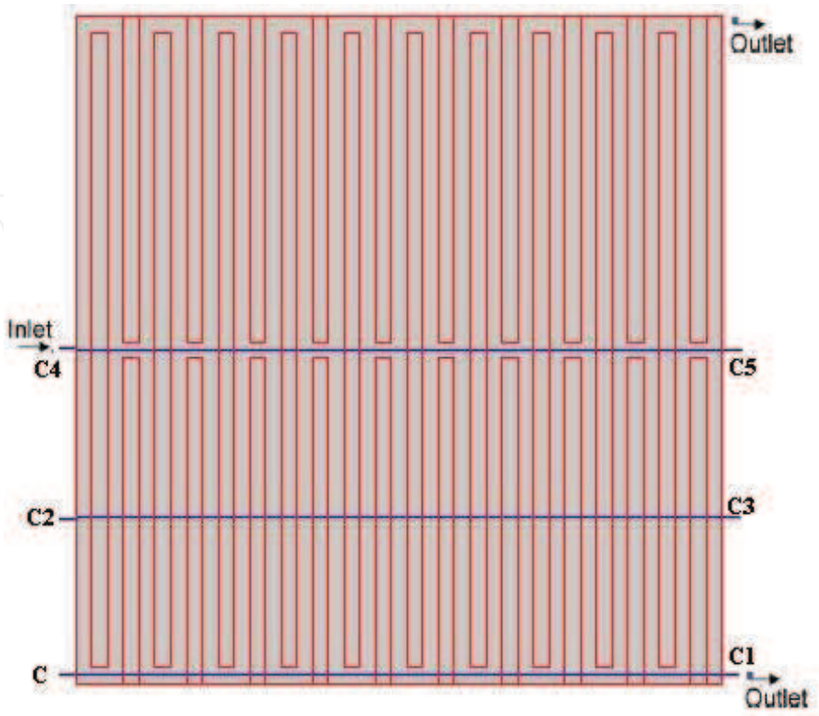


Fig. 2. Biophysical Flow Slab (BFF1). Source: Wang et al., (2010)

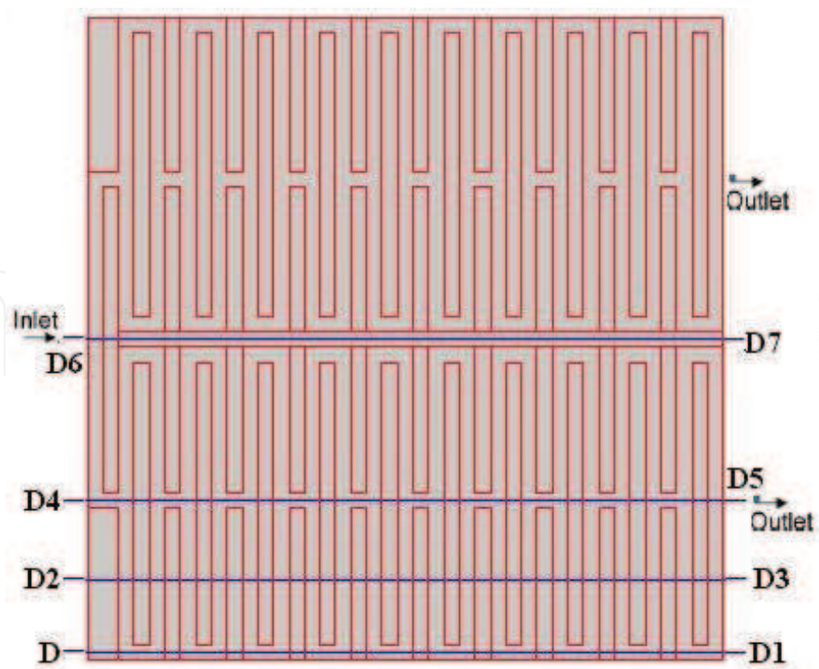


Fig. 3. Biophysical Flow Slab (BFF2). Source: Wang et al., (2010)

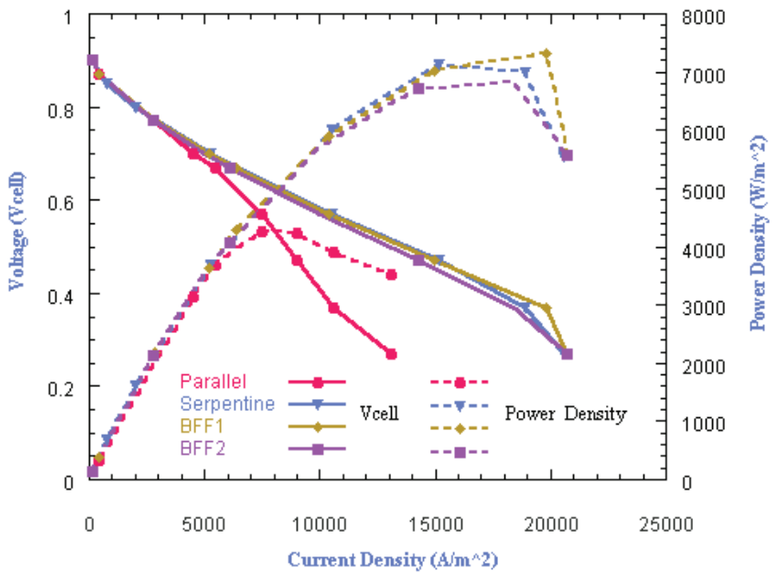


Fig. 4. The *I*–*V*cell and *I*–*W*cell Curves for Types of Parallel, Serpentine, BFF1 and BFF2, respectively.
Source: Wang et al. (2010)

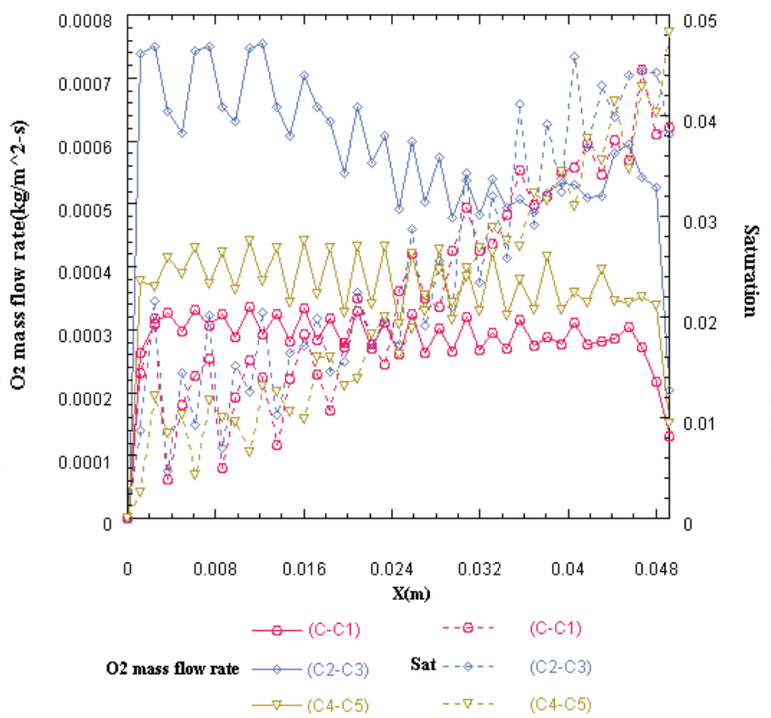


Fig. 5. Oxygen Mass Flow Rate (kgm^{-2}s) and Liquid Water Distributions at the sections of C-C1, C2-C3, C4-C5 Related to 0.7V for BFF1.
Source: Wang et al., (2010)

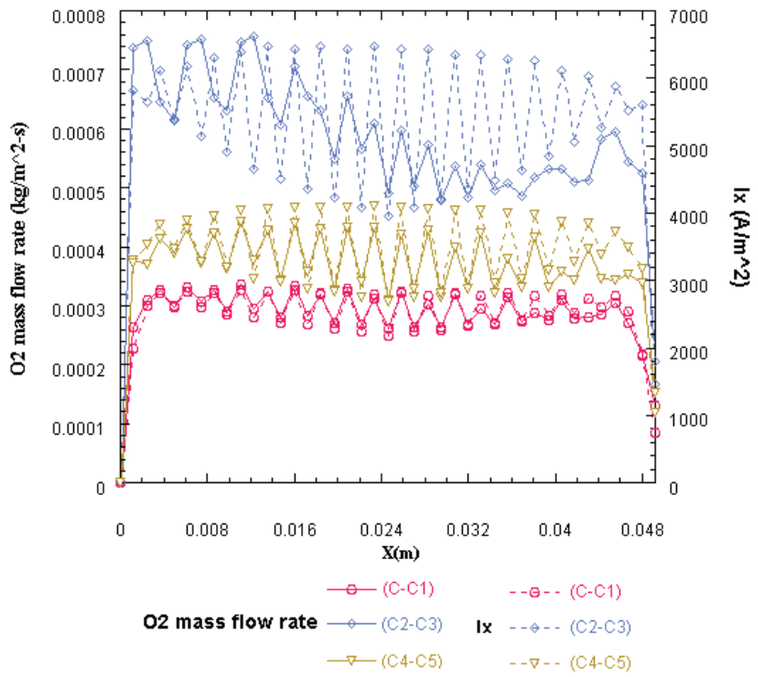


Fig. 6. Oxygen Mass Flow Rate (kgm^{-2} s) and Current Density Distributions (Am^{-2}) at the Sections of C-C1, C2-C3, C4-C5 Related to 0.7V for BFF1.
Source: Wang et al., (2010)

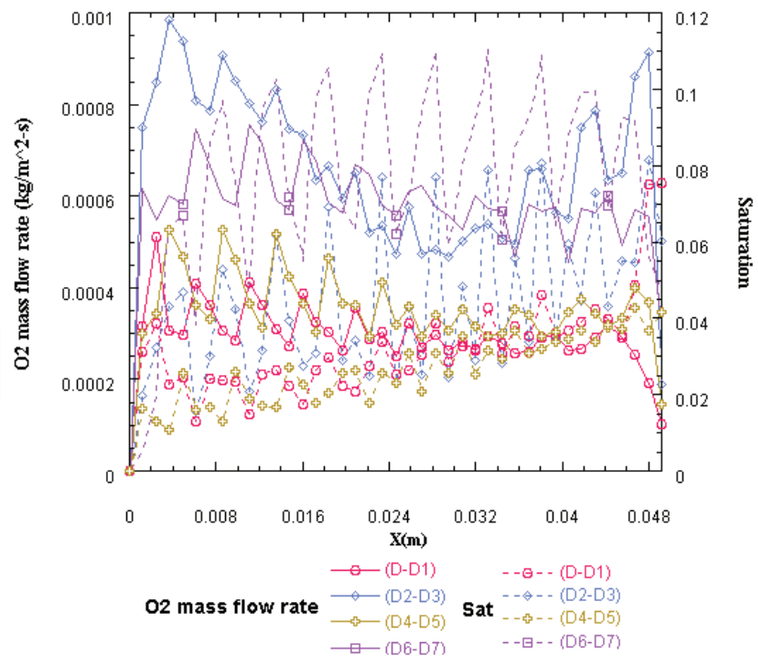


Fig. 7. Oxygen Mass Flow Rate (kgm^{-2} s) and Liquid Water Distributions at the Sections of D-D1, D2-D3, D4-D5, D6-D7 Related to 0.7V for BFF2.
Source: Wang et al., (2010)

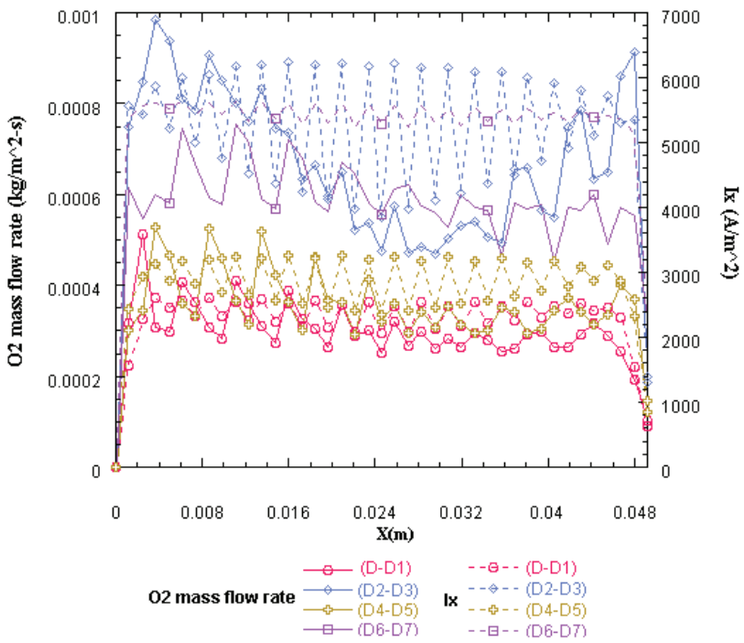


Fig. 8. Oxygen Mass Flow Rate (kgm^{-2} s) and Liquid Water Distributions at the sections of D-D1, D2-D3, D4-D5, D6-D7 Related to 0.7V for BFF2.
Source: Wang et al., (2010)

2.3 Biometric flow slab applied to Microbial Fuel Cells (MFCs) (Wang et al., 2011)

In the academic studies of microbial fuel cells (MFCs), there is a significant absence of sufficient discussion and research regarding to the design of flowchannels and flow-fields (Hameler et al., 2006; Logan et al., 2004), and even less discussion as to why and how they could be applied to MFCs. However, the research of flow channels being applied in fuel cells have been proven to have a significant contribution to power performances (Wang et al., 2009; Sabir et al., 2005), especially with regards to fuel efficiency and power density (Sabir et al., 2005). A new biometric flow channel, shown in Figure 9 and applied in rumen microbial fuel cells (RMFCs), was first addressed by (Wang et al., 2011). Looking at Figure 10 and Table 4, the obstacle groups of No.A and No.C have a higher flow mixing efficiency inside the chamber of RMFCs. The obstacles can cause flow to split and recombine to enhance flow mixing. Since the Reynolds number is higher in the case of No.C, the flow convection at the inlet entrance of RMFCs is more intensive than in the case of No.A and also has a higher flow mixing. In Case No.D, without obstacles, flow separation is created due to a high Reynolds number (Lashkov et al., 1992; Jadhav et al., 2009) and the Coanda effect.

Therefore, proton exchange seems to be unevenly mixed because the main flow and the separation flow are almost without interaction. In addition, the electron and proton from the reactants will continue to be exhausted from the charged reaction of RMFCs, and finally creates a concentration loss in some regions of the chamber. Conversely, Case No.B does not experience that problem because of the lower Reynolds number, thus creating a smoother flow and more even reaction. Even though the flow obstacles do not exhibit noticeable benefits in the flow mixing, the effect on the flow field is overall beneficial to the electricity

system (Wang et al., 2009). This creates a better interaction on the surfaces of electrodes and proton exchange membranes, thus avoiding concentration loss and proving more efficient than flow fields that are uneven. In this study rumen microbes and plant fibers that acted as substrates were utilized in single chambers in the cases of both using obstacles and different Reynolds numbers respectively to investigate the power performance of RMFCs. The RMFC system with a biometric flow channel (with obstacles), and at a higher Reynolds number (Re= 496.18), will produce a higher power performance with a voltage potential and power density of 0.716 V and 0.022mW/m² respectively. This is much better than in the cases without obstacles showing a positive effect of a biometric flow channel on the power performance of RMFCs.

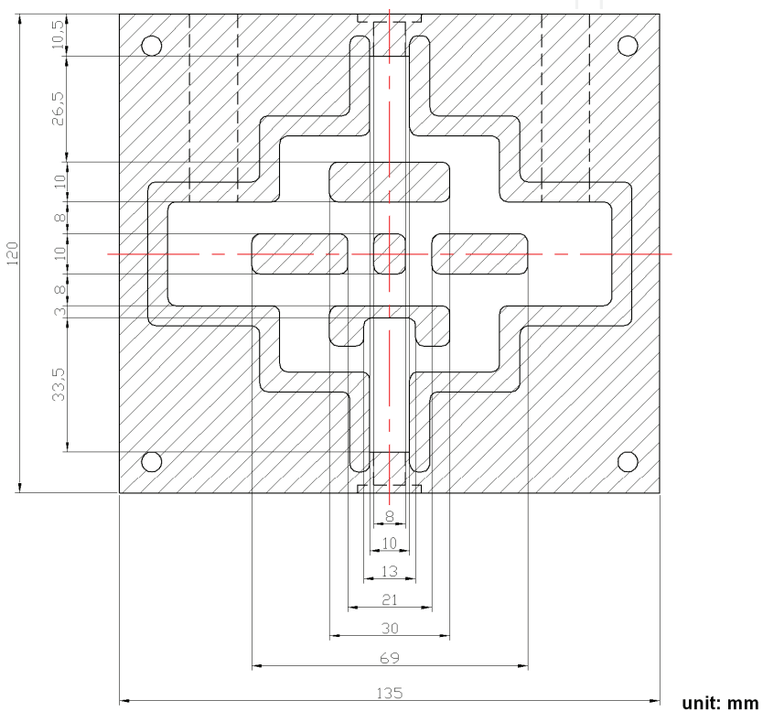


Fig. 9. Geometrical Dimensions of a Biometric Flow Channel for RMFCs. Source: Wang et al., 2011

MFCs	Re No.	Flow mixing efficiency at analyzed positions (%)				
		a	b	c	d	e
No.A	19.85	99.6	99.8	99.8	99.7	99.8
No.B		99.0	99.3	99.0	99.3	99.4
No.C	496.18	99.8	99.8	99.9	99.7	99.9
No.D		100.0	100.0	100.0	100.0	100.0

Table 4. Flow Mixing Efficiency Versus Different Flow Conditions and Cross-sections analyzed.
Source: Wang et al., 2011

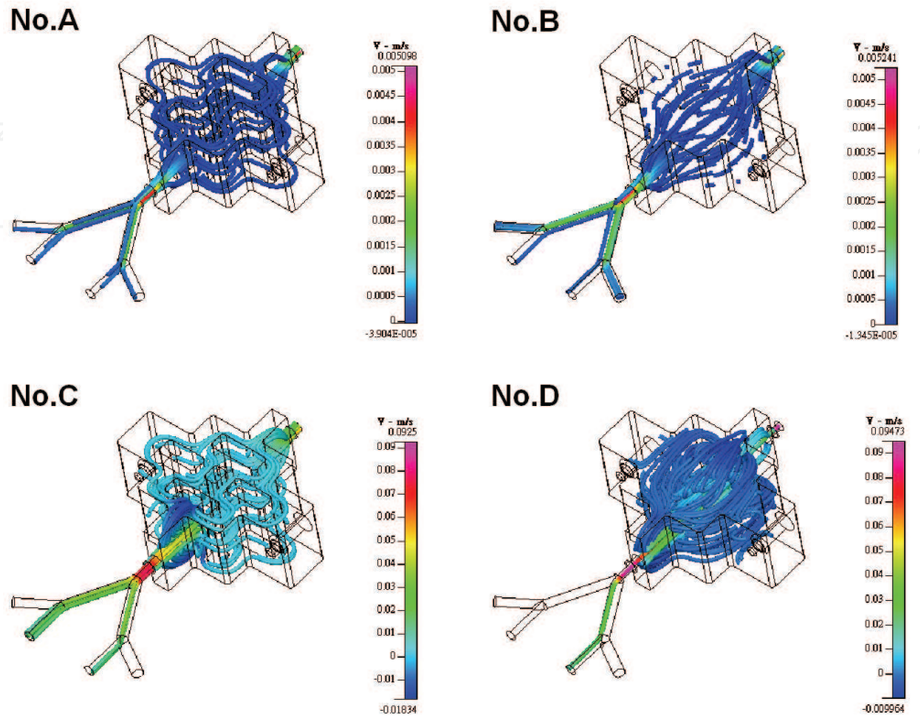


Fig. 10. 3D Flow Velocity Images Versus Different Flow Conditions and Cross-sections Analyzed (shown in Table 4).
Source: Wang et al., 2011

3. Biophysical micro-mixer (Wang et al., 2009)

In this work, a biophysical concept was applied to passive micro-mixers, named as a biophysical micro-mixer and shown in Figure 11, to promote mixing efficiency. The vertical width of a channel would be gradually increased from 20 μm at the inlet to 40 μm at the middle section of the device, and then gradually decreased along the flow downstream to the outlet. During the flow transmission process, the flow would be split first and then recombined with a flow motion. When the flow passes through the middle section of the system, increasing interfaces were created exponentially by laminating the interfaces continuously along the channel. In addition, the convection flow in the biophysical channels had a high flow uniformity and low pressure drop to enhance the flow mixing (shown in Figure 12). The mixing coefficient will approach 0.95 when the Reynolds number of the inlet mid-channel is larger than 160. This result shows that the Reynolds number positively affects mixing although it induces an increase in pressure drop (Wang et al., 2009). Therefore, the prototype of a biophysical micro-mixer is simple and possesses a better

uniformity and lower pressure drop, so it can be expected to be useful to promote the mixing performance of passive micro-mixers when the mixing distance is restricted. These findings will be useful in the design of an optimal biophysical passive micro-mixer in further research. Parameters, such as the Reynolds number ratio and aspect ratio and their effect on mixing and pressure drop, required investigation because finding the optimal Reynolds number ratio, Rer, and aspect ratio, AR, is important for the operation of the micro-mixer.

To address the effect of the different inlet flow conditions on the mixing performance, a parameter denoted as Rer defined in (3) was set for the Reynolds number ratio:

$$\mathrm{Re}_r = \frac{\mathrm{Re}_1 + \mathrm{Re}_3}{\mathrm{Re}_2} \tag{3}$$

Here, the operational Reynolds number defined in (4) was set in the range of Re=0.5 to 10:

$$\mathrm{Re} = \frac{\rho U_{ave} W}{\mu} \tag{4}$$

Where ρ is the density of the fluid, U_{ave} is the average velocity of the inlet channel; W, whose value is 20 μm, represents the width of inlet channel I_2 and the outlet channel. μ is the dynamic viscosity of the working fluid.

In addition, the aspect ratio, AR, ranging from 0.5 to 10 is defined in (5) and was investigated in order to study the sidewall effects on mixing performance:

$$AR = \frac{D}{W} \tag{5}$$

where D is the depth of the channel and W is fixed at 20μm for the inlet at mid-channel.

Hence, the Reynolds number ratio was decided and based on the variations of inlet Reynolds numbers from Re = 0.5 to 10 for the inlet channels. In addition, variations of aspect ratio were set as 0.5, 1, 2 and 10 for determining the sidewall effect on mixing and pressure. The results, shown in the Table 5, are addressed as follows:

First, the optimal Reynolds number ratio was Rer = 0.85, because of its outstanding mixing performance at different aspect ratios. Second, the sidewall effect will influence the variations in pressure drop and mixing performance, and increasing the AR will also decrease the pressure. An optimal aspect ratio with the highest mixing effect was found at AR = 2, which exhibited a good mixing for studied cases. In addition, the inlet angle of the side-channels and its effect on mixing and pressure was considered in the design of the micro-mixer. Hence, a variety of inlet angles of the side-channels, represented by θ, were executed with Reynolds number ratios ranging from Rer = 0.5 to 2 in the case of Re2 = 1 and its relationship to mixing performance and pressure drop are shown in Table 5.

The results of Table 6 show that a side-channel inlet angle of 30° was a better choice because it possesses a better mixing effect and has a lower pressure drop. These findings will be useful in the optimal design of a passive micro-mixer based on biophysical concepts in further experimental studies.

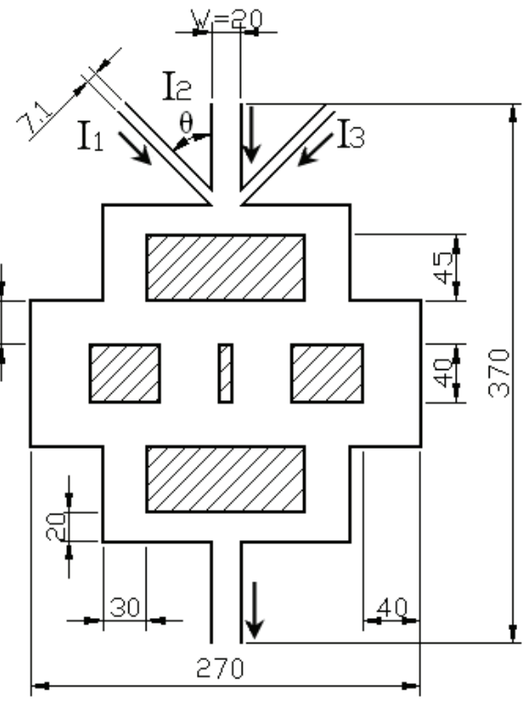


Fig. 11. Prototype of a Biophysical Micro-mixer (unit: μm)
(Arrows indicate the inlet and outlet flow direction).
Source: Wang et al., (2009)

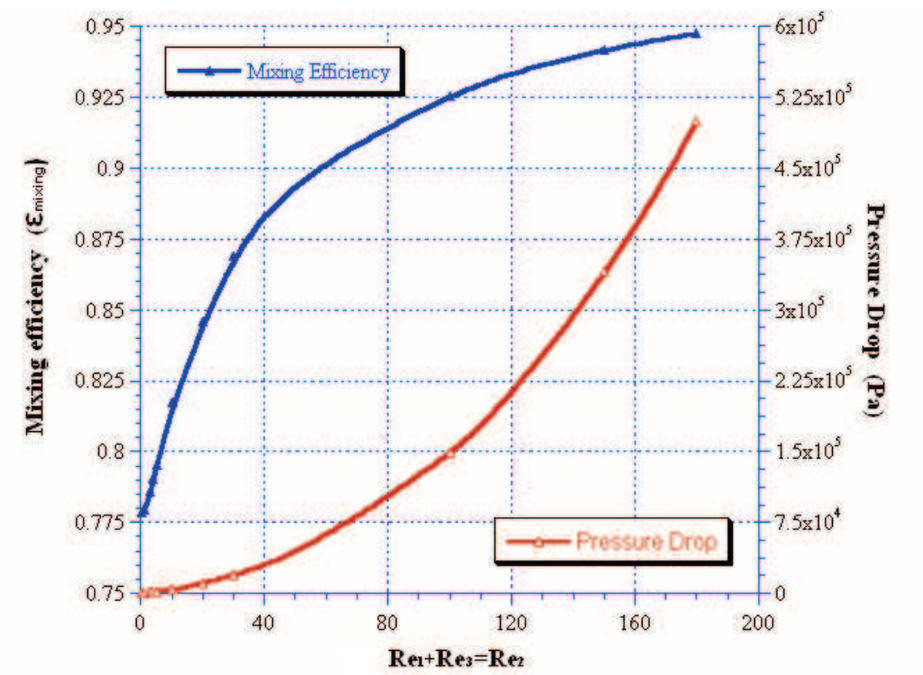


Fig. 12. Reynolds Number Effect Versus the Mixing and Pressure Drop at Rer = 1
Source: Wang et al., (2009)

	Rer	0.5	0.85	1	2	1
	Re1	0.5	0.85	1	2	10
	Re2	1	1	1	1	10
ΔP	AR = 0.5	1890.52	2333.07	2522.87	3790.44	25999.58
ΔP	AR = 1	746.72	922.50	1891.34	1503.66	10908.40
ΔP	AR = 2	449.06	555.37	601.07	908.16	6915.66
ΔP	AR = 10	320.69	396.79	429.52	649.51	4956.02
ε_{mixing}	AR = 0.5	0.72	0.79	0.78	0.61	0.76
ε_{mixing}	AR = 1	0.73	0.79	0.78	0.59	0.80
ε_{mixing}	AR = 2	0.69	0.80	0.80	0.67	0.85
ε_{mixing}	AR = 10	0.73	0.79	0.79	0.62	0.83

Table 5. Variations of Mixing Coefficient (ε_{mixing}) and Pressure Drop (ΔP; unit: Pa) Versus the Reynolds Number Ratio (Rer) and Aspect Ratio (AR).
Source: Wang et al., (2009)

	Rer = 0.5		Rer = 0.85		Rer = 1		Rer = 2	
Inlet angle of side channel, θ	ε_{mixing}	ΔP	ε_{mixing}	ΔP	ε_{mixing}	ΔP	ε_{mixing}	ΔP
90°	0.737	310.901	0.786	384.537	0.771	417.240	0.581	632.116
60°	0.738	300.758	0.791	371.628	0.776	403.076	0.580	609.910
45°	0.739	300.025	0.796	371.122	0.779	401.692	0.584	607.082
30°	0.738	300.781	0.803	371.240	0.790	402.526	0.589	607.998
0°	0.729	289.187	0.764	356.386	0.750	385.829	0.575	586.702

Table 6. Inlet Angle of Side-channel Versus the Mixing (ε_{mixing}) and Pressure Drop (ΔP; unit: Pa) with Variations of Reynolds Number Ratios ranging from Rer = 0.5 to 2 in the case of $Re_2 = 1$.
Source: Wang et al., (2009)

4. Conclusion

In this chapter, the biometric concept was applied to the fuel cells, microbial fuel cells and micro-mixer. To sum up, some results are addressed as follows:

In the study of a biometric fuel cell, the novel flow slab provides a better performance when using the bionic concept because it can control the velocity distribution, pressure drop, coupling effect and has a stronger ability to remove the liquid water and so providing a better power performance of cells. These findings, with respect to a biometric flow slab, would be useful to improve PEMFCs and could even be expanded to other types of cells. In addition, a new design of biometric flow channel was also applied to RMFCs. Experiments in a circulation system were executed by using a double two-inlet Y-type inlet channel and connecting it with the RMFCs. The biometric flow channel would create a more uniform flow field with obstacles than one without, regardless of the Reynolds number. An extra voltage output of 0.2 V, based on the example without obstacles, was provided as in the case of the one with. This further explains the design of biometric flow channels having a greater, more positive effect on power performance.

In the study of the biometric micro-mixer**,** a novel micro-mixer design based on the biophysical concept was addressed. The prototype was simple and possessed a better flow uniformity and lower pressure drop, so it could be expected to be useful to promote the mixing performance of passive micro-mixers when the mixing distance was restricted. The highest mixing coefficient with ε_{mixing} = 0.876 occurred at a Reynolds number ratio, Rer = 0.85. These findings will be useful in the design of an optimal biophysical passive micro-mixer in future research and even show the feasibility and potential of the biometric concept widely applied in biochemical, biological andchemical analysis, along with fuel cells and bioenergy.

5. References

A. Ter Heijne, H.V.M. Hamelers, V. De Wilde, R.A. Rozendal and C.J.N. Buisman. (2006) A bipolar membrane combined with ferric iron reduction as an efficient cathode system in microbial fuel cells. *Environ. Sci. Technol,* Vol. 40：5200-5205.

A. Y. Lashkov, I. N. Sokolova and E. A. Shumilkina. (1992) Jet flow over ribbed curved surfaces. *Fluid Dynamics*, Vol.27 (1) ：135-137.

Bayer, T., Himmler, K., Hessel, V. (2003) Don't be baffled by static mixers. *Chemical Engineerinf*, Vol. 5：2-9.

B. Min and B.E. Logan. (2004) Continuous electricity generation from domestic wastewater and organic substrates in a flat plate microbial fuel cell. *Environ. Sci. Technol,* Vol. 38：5809-5814.

Dumas, C., Basseguy, R., Bergel, A. (2008) DSA to grow electrochemically active biofilms of Geobacter sulfurreducens. *Electrochimica Acta*, Vol. 53：3200-3209.

Ehrfeld, W., Hessel, V., Lowe, H. (2000) Microreactors. *Wiley-VCH*, Weinheim.

G.S. Jadhav and M.M. Ghangrekar. (2009) Performance of microbial fuel cell subjected to variation in pH, temperature, external load and substrate concentration. *Bioresour. Technol,* Vol. 100 ： 717-723.

Hessel, V., Hardt, S., Lowe, H. (2004) Chemical Micro Process Engineering-Fundamentals, Modelling and Reactions. *Wiley-VCH*, Weinheim.

Jensen, K. F. (1998) Smaller, faster chemistry, *Nature.* Vol. 393 (6) ：735-736.

Johnson, S. W., Aref, H. (1998) Chaotic advection in pulsed source-sink systems. *Physics of Fluids*, Vol. 31：469-485.

Kamholz, A. E., Yager, P. (2002) Molecular diffusive scaling laws in pressure-driving nicrofluidic channels: deviation from one-dimensional Einstein approximations. *Sensors and Actuators B*. Vol. 82(1) ：117-121.

Kloess J. P., Wang X., Liu J., Shi Z.& Guessous L. (2009) Investigation of bio-inspired flow channel designs for bipolar plates in PEM fuel cells. *J Power Sources*, Vol.188 (1)：132-140.

Lovely, D. R. (2008) The microbe electric: conversion of organis matter to electricity. *Curr Opin Biotech-nol*, Vol. 19 ：564-571.

Lowe, H., et al., (2000) Micromixing technology. *In: Fourth International Conference on Microreaction Technology*, IMRET 4, Atlanta, USA. Ai.I. Ch. E. Topic Conference Proceedings：31-47.

Maeng, J. S., Yoo, K., Song, S. (2006) Modeling for fluid mixing in passive micromixers using the vortex index. Journal of the Korean Physical Soceity, Vol. 48 (5) ：902-907.

Marsala G., Pucci M., Vitale G., Cirrincione M.& Miraoui A.(2009) A prototype of a fuelcell PEM emulator based on a buck converter. *Appl Energ*, Vol. 86：2192-2203.

Mei S. C., Yan W. M. , Yang C. H. , Soong C.Y. & Chen F.(2006) Experimental studies on optimal operating conditions for different flow field designs of PEM fuel cells. *J Power Sources*, Vol.160：284–292.

Nguyen, N. T., Wu, Z. (2005) Micromixers-a review. *J. Micromech. Microeng*. Vol. 15, Vol. 15：R1-R6.

Perng, S. W., Wu, H. W., Jue, T. C., Cheng, K. C. (2009) Numerical predictions of a PEM fuel cell performance enhancement by a rectangular cylinder installed transversely in the flow channel. *Apply Energy*. Vol. 86(10) ：2192-2203.

X. Li and I. Sabir. (2005) Review of bipolar plates in PEM fuel cells: Flow-field designs. *Int. J. Hydrogen Energy*, Vol. 30：359-371.

Wang X.D., Duan Y. Y. & Yan W. M.(2007) Novel serpentine-baffle flow field design for proton exchange membrane fuel cells. *J Power Sources*, Vol. 173：210–221.

Perng S.W., Wu H.W., Jue T.C.& Kuo-Chih Cheng. (2009) Numerical predictions of a PEM fuel cell performance enhancement by a rectangular cylinder installed transversely in the flow channel. *Appl Energ*, Vol. 86 (10)：2192-2203.

Wang C. T., Chang P. C., Shaw C. K. & Cheng J. Y. (2009) Fuel cell bionic flow slab design. *J. Fuel Cell Sci. Technol*, Vol.6：1-5.

Wang C. T., Hu Y. C. & Zheng P. L. (2010) Novel Biometric Flow Slab Design for Improvement of PEMFC Performance, *Applied Energy*, Vol.87：1366-1375.

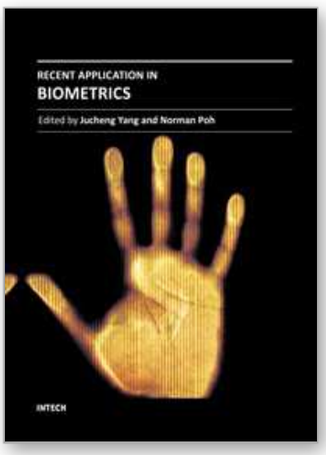
Wang C. T., Hu Y. C. and Hu T.Y. (2009) Biophysical Micromixer. *Sensors*, Vol. 9：5379-5389.

Wang, C. T., Yang, C. M., Chen, Z. S., Tseng S. (2011) Effect of Biometric Flow Channel on the Power Generation at Different Reynolds Numbers in the Single Chamber of Rumen Microbial Fuel Cells (RMFCs). *International Journal of Hydrogen Energy*, Vol.36 : 9242-9251

Watanabe, K. (2008) Recent developments in microbial fuel cell technologies for sustainable bioenergy, *J Biosci Bioeng*, Vol. 106：528-536.

Wong, S.H.; Bryant, P.; Ward, M.& Wharton, C. (2003) Investigation of mixing in a cross-shaped micro-mixer with static mixing elements for reaction kinetics studies sens. *Sens. Actuat. B - Chem.*, Vol. *95*：.414-424.

IntechOpen



Recent Application in Biometrics
Edited by Dr. Jucheng Yang

ISBN 978-953-307-488-7
Hard cover, 302 pages
Publisher InTech
Published online 27, July, 2011
Published in print edition July, 2011

In the recent years, a number of recognition and authentication systems based on biometric measurements have been proposed. Algorithms and sensors have been developed to acquire and process many different biometric traits. Moreover, the biometric technology is being used in novel ways, with potential commercial and practical implications to our daily activities. The key objective of the book is to provide a collection of comprehensive references on some recent theoretical development as well as novel applications in biometrics. The topics covered in this book reflect well both aspects of development. They include biometric sample quality, privacy preserving and cancellable biometrics, contactless biometrics, novel and unconventional biometrics, and the technical challenges in implementing the technology in portable devices. The book consists of 15 chapters. It is divided into four sections, namely, biometric applications on mobile platforms, cancelable biometrics, biometric encryption, and other applications. The book was reviewed by editors Dr. Jucheng Yang and Dr. Norman Poh. We deeply appreciate the efforts of our guest editors: Dr. Girija Chetty, Dr. Loris Nanni, Dr. Jianjiang Feng, Dr. Dongsun Park and Dr. Sook Yoon, as well as a number of anonymous reviewers.

How to reference
In order to correctly reference this scholarly work, feel free to copy and paste the following:

Chin-Tsan Wang (2011). Biometric application in fuel cells and micro-mixers, Recent Application in Biometrics, Dr. Jucheng Yang (Ed.), ISBN: 978-953-307-488-7, InTech, Available from: http://www.intechopen.com/books/recent-application-in-biometrics/biometric-application-in-fuel-cells-and-micro-mixers

INTECH
open science | open minds

InTech Europe
University Campus STeP Ri
Slavka Krautzeka 83/A
51000 Rijeka, Croatia
Phone: +385 (51) 770 447
Fax: +385 (51) 686 166
www.intechopen.com

InTech China
Unit 405, Office Block, Hotel Equatorial Shanghai
No.65, Yan An Road (West), Shanghai, 200040, China
中国上海市延安西路65号上海国际贵都大饭店办公楼405单元
Phone: +86-21-62489820
Fax: +86-21-62489821

© 2011 The Author(s). Licensee IntechOpen. This chapter is distributed under the terms of the Creative Commons Attribution-NonCommercial-ShareAlike-3.0 License, which permits use, distribution and reproduction for non-commercial purposes, provided the original is properly cited and derivative works building on this content are distributed under the same license.

IntechOpen

IntechOpen